ELSEVIER

Journal of Materials Processing Technology 178 (2006) 128–134

Journal of Materials Processing Technology

www.elsevier.com/locate/jmatprotec

Quantification of the microconstituents formed during solidification by the Newton thermal analysis method

H. Cruz [a,*], C. Gonzalez [a], A. Juárez [b], M. Herrera [c], J. Juarez [d]

[a] *Departamento de Ingeniería Metalúrgica, Facultad de Química, UNAM, Circuito Exterior S/N, Edif. "D", Cd. Universitaria, 04510 México D.F., Mexico*

[b] *CIATEQ A.C. Calz. Del Retablo 150, Col. Fovissste, 76150 Querétaro Qro., Mexico*

[c] *CINVESTAV, IPN, Unidad Saltillo, Carretera Saltillo-Monterrey Km 13, 25000 Saltillo Coahuila, Mexico*

[d] *Instituto de Investigaciones en Materiales, UNAM, Circuito Exterior S/N, Cd. Universitaria, 04510 México D.F., Mexico*

Received 8 July 2004; received in revised form 1 December 2005; accepted 9 March 2006

Abstract

This work was intended to explore the reliability of the Newtonian thermal analysis method as a tool for the quantification of the amount of alloy microconstituents formed during solidification as observed at room temperature in alloy systems without phase transformations in the solid state. This technique was applied to three hyper eutectic Pb–Sn alloys with different primary phase content using different approaches to determine the time of start of solidification and for the zero curve calculation. Quantitative metallography was used to determine the primary phase content in the experimental probes. The outcome of this work shows that the use of Newton method for prediction of the amount of microconstituents formed during solidification obtain good results in two of the three cases under study suggesting that this method is not reliable.

Keywords: Cooling curve analysis; Microconstituent quantification

1. Introduction

Cooling curve analysis has become a common tool for the control of microstructural characteristics of cast alloys. This technique involves the monitoring of the temperature changes in a melt during its cooling and solidification. Usually, it is represented by a temperature–time cooling curve and its derivative. During solidification the latent heat released by the solidifying microconstituents causes changes in the cooling curve and its derivative which are linked with the development and characteristics of the microstructure observed in the cast product. The correlation among the changes observed in the cooling curve and its derivative and the microstructure present in the cast by statistically based models [1] has allowed the foundryman to monitor and control the melt quality before pouring. In this regard, there have been several efforts focused to extend the conventional analysis of cooling curves in order to obtain a more detailed picture of the events occurring during solidification.

It has been shown [2] that the numerical processing of cooling curves by the so called computer aided cooling curve analysis methods (CA-CCA) [2–6] can be used to generate information about solidification kinetics and latent heat released during solidification.

The simplest method of CA-CCA is the Newton thermal analysis method (NTA) [2]. This method is based on the assumption of the absence of thermal gradients inside the sample during the cooling process, enabling the generation of quantitative data that describes the solidification of the sample from the numerical processing of a cooling curve obtained from the reading of one thermocouple located at the thermal centre of the cast. NTA method has shown to be capable to obtain quantitative information regarding the latent heat of solidification, the solidification kinetics and also it has been claimed to allow the determination of the amount of microconstituents formed during solidification.

One of the most promissory applications of CA-CCA is the quantification of the amounts of microconstituents present in solidified alloys from the numerical processing of cooling curves, due to its potential impact in process control. Nevertheless, there are few works [7,8] focused in this regard.

* Corresponding author.
E-mail addresses: carlosgr@servidor.unam.mx (H. Cruz), mherrera@saltillo.cinvestav.mx (M. Herrera), julioalb@servidor.unam.mx (J. Juarez).

0924-0136/$ – see front matter © 2006 Elsevier B.V. All rights reserved.
doi:10.1016/j.jmatprotec.2006.03.152

The purposes of this work are:

- To explore the reliability of NTA method as a tool for the quantification of solidified microconstituents from the numerical processing of cooling curves and quantitative image analysis.
- To compare different approaches that can be used to implement NTA in order to identify the methodology that obtains the best results regarding quantification of microconstituents.

2. Newton thermal analysis

NTA thermal analysis method assumes the absence of thermal gradients within the melt under study, during its cooling and solidification. From this the energy balance by unit volume applied to the melt can be written as:

$$\frac{Q_{ex}}{M} + L_F \frac{df_s}{dt} = C_v \frac{dT}{dt} \quad (1)$$

where Q_{ex} is the heat flux (W/m^2) transferred from the melt to the surrounding mould, M the modulus of the cast (m), L_F the volumetric latent heat of fusion (J/m^3), f_s the solid fraction, df_s/dt (s^{-1}) the rate of solidification, C_v the volumetric heat capacity of the melt (J/(m^3 °C)) and dT/dt is the cooling rate (°C/s). Eq. (1) can be described in terms of the volumetric heat flows (W/m^3) present in the system:

$$Q_c + Q_s = Q_a \quad (2)$$

where Q_c is the instantaneous volumetric heat flow transferred from the melt to the surrounding mould, Q_s the volumetric flow of latent heat released by solidification and Q_a is the volumetric flow accumulated within the melt. Eq. (1) can be rearranged in terms of Q_s:

$$Q_s = C_v \frac{dT}{dt} - \frac{Q_{ex}}{M} = C_v \left(\frac{dT}{dt} - ZN \right) \quad (3)$$

Eq. (3) shows the foundation of NTA method, which consist in the calculation, during solidification, of the difference between the first derivative of the experimental cooling curve, dT/dt and an hypothetical cooling rate evolution, called zero or baseline curve, ZN which indicates the cooling rate evolution that the system would show if the latent heat released from the solidification of the real system were not present. Before the time of start, t_{ss} and after the time of end, t_{es}, of solidification $Q_s = 0$ and Eq. (3) shows that there is a ZN characteristic for the liquid and for the solid state of the melt, numerically equal to the corresponding dT/dt evolution near t_{ss} and t_{es}.

Some procedures applied to the implementation of NTA method have been described elsewhere [2,4,6] and starts with the numerical processing of the cooling curve to obtain its derivative, followed by the location of the times of start and end of solidification and the generation of ZN. In this regard, there have been several proposals for the ZN calculation, which have been described and evaluated [4] finding that the best results regarding latent heat quantification are reached when the characteristic values of ZN before and after solidification are considered for the generation of ZN curve.

Once ZN and dT/dt are known in the time interval between t_{ss} and t_{es}, the instantaneous volumetric heat released by solidification, Q_s, is calculated using Eq. (3).

The latent heat of solidification of the melt is obtained from the integration of Q_s as:

$$L_F = \int_{t_{ss}}^{t_{es}} C_v \left(\frac{dT}{dt} - ZN \right) dt \quad (4)$$

The solid fraction at time t is calculated as:

$$f_s = \frac{1}{L_F} \int_{t_{ss}}^{t} C_v \left(\frac{dT}{dt} - ZN \right) dt \quad (5)$$

In alloy systems where there are two main solidification microconstituents, a primary phase and an eutectic which starts its solidification at time t_{se}, time of start of eutectic solidification, the volume fraction of primary phase, f_{pp}, can be calculated according with:

$$f_{pp} = \frac{1}{L_F} \int_{t_{ss}}^{t_{se}} C_v \left(\frac{dT}{dt} - ZN \right) dt \quad (6)$$

and the volume fraction of eutectic microconstituent can be obtained as:

$$f_{eu} = 1 - f_{pp} \quad (7)$$

It can be mentioned that this procedure could be extended to three or more solidified microconstituents and the problem could be to differentiate between the energetic contributions of each of them when there is simultaneous growth. Some efforts to accomplish this goal have been described in the case of Cu-bearing phases in Al-based alloys [8].

The key features of NTA method focused on the analysis of this kind of systems are the determination of the times of start and end of solidification, the time of start of eutectic solidification and the generation of the zero curve. In most of the papers focused on NTA method there is a lack of clarity on some procedures that need to be applied in order to calculate these parameters. Accordingly, different procedures to calculate these parameters are analysed in this work in order to identify a methodology focused on the quantification of the microconstituents formed during solidification in the case of the presence of a primary phase and an eutectic microconstituent.

3. Determination of t_{ss}, t_{es} and t_{se}

NTA procedure is performed on the first derivative of the cooling curve, see Fig. 1(a). It can be seen in this figure that, following a first stage of thermal stabilisation of the thermocouple which ends at the first minimum observed on dT/dt curve, the first derivative shows a gradual evolution to less negative values, with a trend which shows a concave downwards shape, region 1, which corresponds to the cooling of the liquid.

This trend continues until the start of solidification, which occurs near to point "a", when the release of the latent heat starts and causes the sharp increase of the derivative to positive values, region 2, until a maximum is reached, point "b". After this moment it can be observed a decrease, first rapidly, region 3,

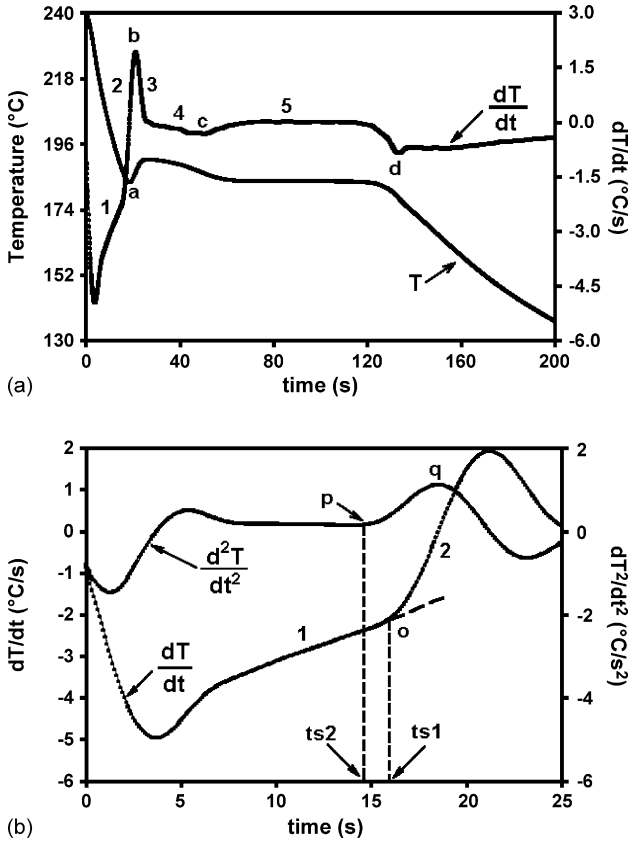

Fig. 1. (a and b) First and second derivative of a cooling curve showing the relevant features considered for t_{ss} determination.

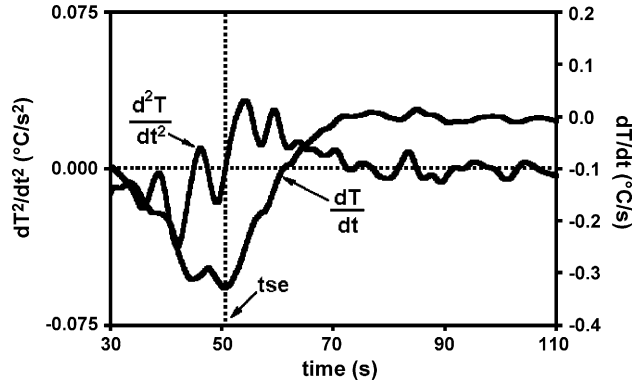

Fig. 2. First and second derivatives of a cooling curve showing the determination of the time of start of eutectic solidification.

and later in a less stepped way of the trend shown by this parameter, region 4, until the curve shows another sudden increase of the derivative to positive values, point "c", associated with the latent heat released by the eutectic in its first stages of solidification. The solidification of the eutectic continues in region 5 until a minimum is registered, point "d", when solidification reaches the end.

With regard to t_{ss} determination two approaches (which will be named ts1 and ts2 procedures) will be considered. After the stage of cooling of the liquid, region 1 near to point "a", Fig. 1(a), it can be detected on the first derivative a change in its trend to more positive values, present at the beginning of the region 2, near to point "a", Fig. 1(a) as a result of the release of latent heat at the beginning of solidification. A closer analysis of this zone, Fig. 1(b), shows two different behaviours of the derivative. The first approach for t_{ss} determination (ts1 procedure) is carried out by fitting linearly the last points of region 1 and defining t_{ss} as the point where the dT/dt curve clearly deviates from this trend, see Fig. 1(b), point "o". The change in behaviour of the melt near to point "o" of Fig. 1(b), is associated with the start of solidification and the related thermal indication of the beginning of the latent heat release could be determined more precisely by using the second derivative. The second approach for t_{ss} determination (ts2 procedure) is accomplished in two steps: (1) locate the interval of time in the first derivative where it is observed the change in the initial trend to more positive values, after thermocouple readings stabilisation, until the maximum is reached, region near to point "a", Fig. 1(a); (2) calculate the second derivative of the cooling curve in this region. Second derivative shows a sudden change, point "p", Fig. 1(b) with a notorious increase to more positive values until the reaching of a maximum, point "q". The second procedure considers t_{ss} as the time associated with the beginning of the ascendant trend in the second derivative, point "p", before the maximum "q" is reached, see Fig. 1(b).

In order to know t_{es}, the time of end of solidification, it was followed the commonly used procedure [2] which locates this time at the minimum, see point "d", Fig. 1(a), before that the first derivative shows the final stabilisation in its trend. It has been mentioned that this point not necessarily corresponds with the actual end of solidification but this point is usually very easy to locate, which enhance the reproducibility of the method, see Fig. 1(a).

The time of start of eutectic solidification is identified in two steps: (1) in the first derivative versus time curve, it is needed to locate, following the evolution described for Fig. 1(a), the interval of time where it is observed a sudden increase of the first derivative, i.e. the region around point "c", Fig. 1(a); (2) from the second derivative of the cooling curve calculated within this interval of time, it must be located the time when there is change of sign, from negative to positive values. The time corresponding to this point is assumed to be t_{se}, see Fig. 2.

The volumetric heat capacity of the solid–liquid system during solidification is calculated using a mean value obtained as a function of the operating solid fraction. The values of density and heat capacity of the alloy, shown in Table 1, when it is liquid, ρ_L and Cp_L, at the liquidus temperature and when it is solid, ρ_S and Cp_S at the eutectic temperature are used for this purpose as:

$$C_v = \rho_L Cp_L(1 - f_s) + \rho_S Cp_S(f_s) \quad (8)$$

4. Determination of the baseline curve

Regarding the generation of the zero baseline curve, four approaches (ZN1, ZN2, ZN3 and ZN4 procedures) have been considered. The first approach, ZN1 is obtained from the numerical fitting of the cooling curve after and before solidification [4], in order to obtain the numerical coefficients of equations of the

Table 1
Thermophysical properties considered during calculations

Alloy	T_L (°C)	ρ_L (kg/m^3)	Cp_L (J/(kg °C))	T_E (°C)	ρ_S (kg/m^3)	Cp_S (J/(kg °C))	Reference
Pb–71.5%Sn	194	7973	261	183	8048	219	[9,10]
Pb–77.5%Sn	200	7837	267	183	7920	226	[9,10]
Pb–88.0%Sn	213	7454	276	183	7580	239	[9,10]

type described in Eq. (9)

$$T = a + b\ \exp(-ct) \tag{9}$$

For this purpose two sections of the cooling curve, one corresponding to the cooling of the liquid before the solidification start and the other to the cooling of the solid after the end of solidification are numerically processed. The fitting is performed taking into account the experimental cooling curve points corresponding to 5% of the local solidification time before t_{ss} and after t_{es} using a frequency of acquisition of 10 Hz.

Eq. (9) is derived with respect to time to generate two functions describing, respectively, the liquid, ZN_L and the solid ZN_S behaviour. During solidification ZN is calculated as:

$$ZN = ZN_L(1 - f_s) + ZN_S f_s \tag{10}$$

For the ZN2 and ZN3 approaches it is assumed that, once t_{ss} and t_{es} are known, the associated values of dT/dt are taken, respectively, accordingly with Eq. (3), as representatives of ZN_L, the zero curve value of the liquid at the beginning of solidification, and ZN_S, the zero curve value of the solid state of the system at the end of solidification [2]. The second approach (ZN2 procedure) generates the zero curve by exponential interpolation of the cooling rate curve between the points associated with the start and the end of solidification, assuming a cooling rate behaviour following an equation of the type:

$$\frac{dT}{dt} = X\ \exp(Yt) \tag{11}$$

Using the numerical values associated with the points of start and end of solidification, the constants X and Y can be evaluated and the zero curve can be generated.

For the third approach (ZN3 procedure) and during solidification ZN is calculated using Eq. (10) and the first derivative values corresponding with the times of start and end of solidification.

As the solid fraction is not known at the beginning of the numerical processing of the cooling curve, to start the calculation, it is assumed a linear behaviour of fs between t_{ss} ($f_s = 0$) and t_{es} ($f_s = 1$). This is followed by an iterative procedure until the convergence of the latent heat of solidification calculated by the numerical procedure is reached.

In the case of the ZN4 approach it has been used a procedure which is described in detail elsewhere [11]. The method is based on the measured cooling curve, T versus t and the numerically calculated first derivative dT/dt versus t. From these files it is obtained the plot of dT/dt versus T. The points corresponding to the perturbations associated with initial temperature stabilisation and solidification are eliminated and the numerical fitting of the remaining plot allows obtaining the coefficients of the polynomial function described in Eq. (11):

$$\frac{dT}{dt} = a_0 + a_1 T + a_2 T^2 + a_3 T^3 \tag{12}$$

Eq. (12) is used to generate the baseline in the time interval from t_{ss} and t_{es} using the experimental cooling curve.

Taking into account the two procedures for t_{ss} determination and the four methods for ZN baseline curve generation considered in this work there are eight general procedures that can be applied to the numerical treatment of experimental cooling curves in order to predict the amount of the microconstituents formed during solidification. These procedures are enlisted in Table 2.

Table 2
Selected general procedures used for NTA implementation

Procedure	t_{ss} Determination	ZN generation
1	ts1	ZN1
2	ts2	ZN1
3	ts1	ZN2
4	ts2	ZN2
5	ts1	ZN3
6	ts2	ZN3
7	ts1	ZN4
8	ts2	ZN4

5. Experimental

In order to obtain three hyper eutectic Pb–Sn alloys with different primary phase content, preweighted quantities of 99.8 wt% Pb and 99.9 wt% Sn were melted in an electric furnace with an argon atmosphere to achieve Sn contents in the Pb–Sn alloys of 71.5, 77.5 and 88 wt% Sn. Cooling curves

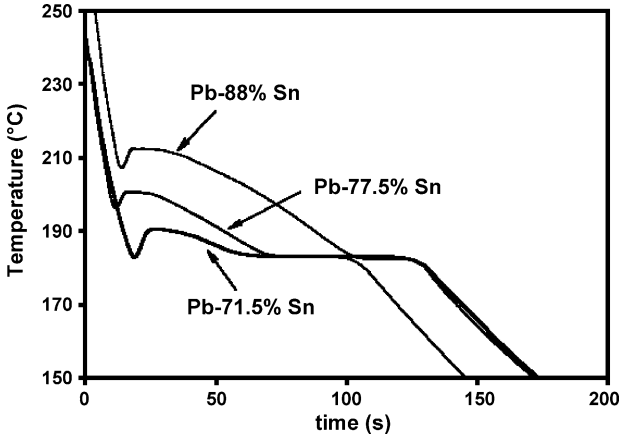

Fig. 3. Cooling curves associated with the Pb–Sn hyper eutectic alloys considered in this work.

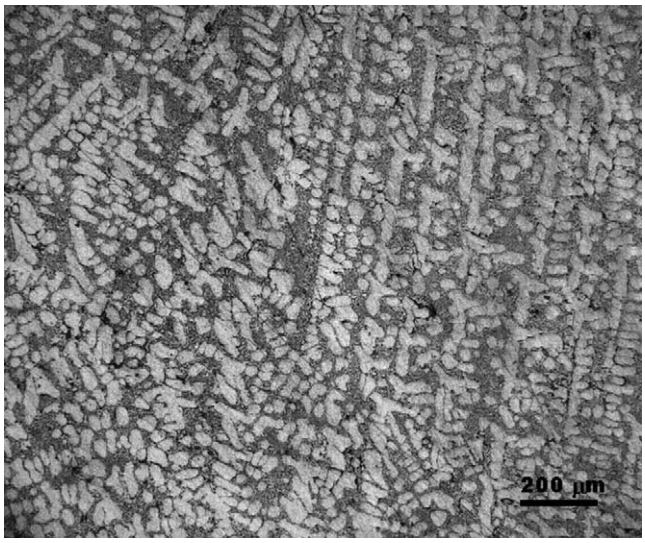

Fig. 4. Microstructure associated with Pb–71.5%Sn.

(a)

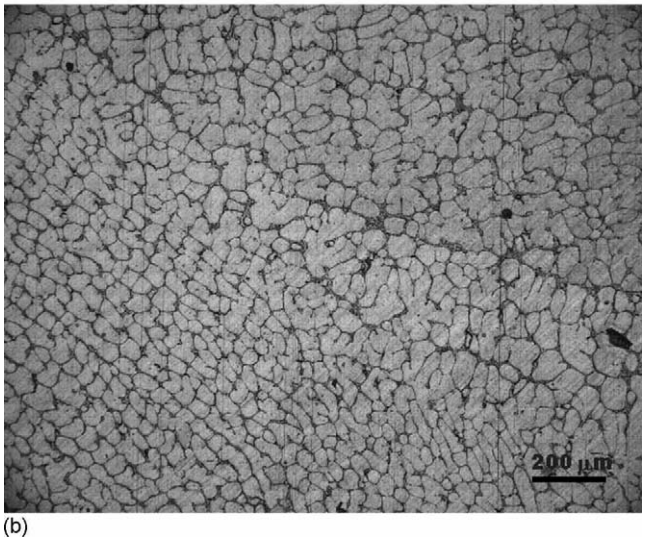

(b)

Fig. 5. Microstuctures associated with (a) Pb–77.5%Sn and (b) Pb–88.0%Sn alloys.

Table 3
Pouring temperatures for the alloys under study

Alloy	Pb–71.5%Sn	Pb–77.5%Sn	Pb–88%Sn
T_P (°C)	295	305	315

for each composition were recorded by triplicate in order to calculate a confidence interval related to the primary phase content present in a specific alloy.

Predetermined quantities of the molten alloys were poured with minimum turbulence directly into silicate/CO_2 bonded sand moulds, with a 25 mm inner diameter, 150 mm in height and 40 mm wall thickness, with isolated top and bottom, and surrounded with silica sand into a moulding box. The pouring temperatures of the alloys of interest are shown in Table 3.

In order to record the thermal history of the alloys during cooling, a type K thermocouple was always located at the same distance of 5 cm from the bottom of the mould symmetry axis to ensure reproducibility of the analysis. The thermocouple tip was in direct contact with the melts under study. The cooling curves were obtained by recording the temperature change as a function of time using a data acquisition system. A calibration procedure [12] was performed with 99.9% Sn after each experiment.

The solidified rods were cut close to the tip of the thermocouple. The cross-sections of the specimens were metallographically prepared and the amounts of microconstituents were measured using optical microscopy and an image analysis system. At least 30 fields were analysed across the sample to establish the percentages of primary phase and eutectic in each probe.

The experimental cooling curves were numerically processed by using the procedures described above regarding t_{ss} and the zero base line determinations

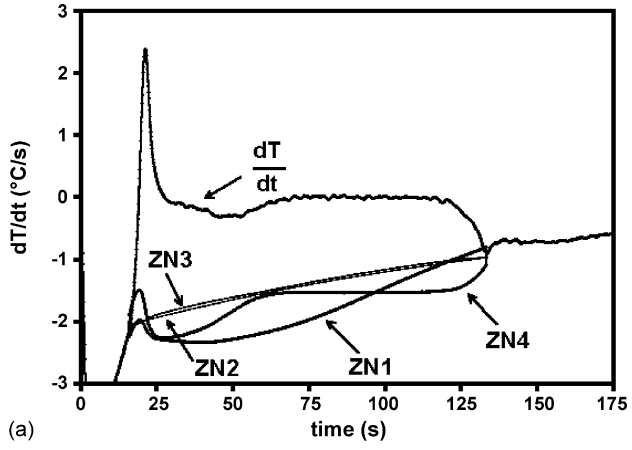

(a)

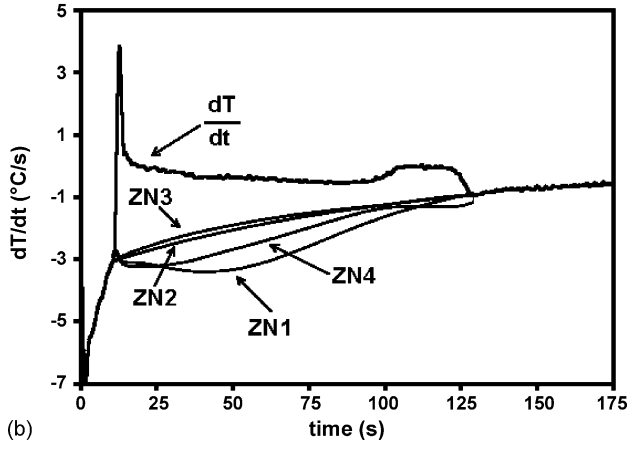

(b)

Fig. 6. First derivative and ZN proposed curves associated (a) with Pb–71.5%Sn alloy and (b) 88% Sn.

shown in Table 2 in order to elucidate the procedures best suited for the prediction of the amount of microconstituents formed during solidification.

6. Results and discussion

Fig. 3 shows the typical cooling curves associated with the cases of interest in this work, where it can be seen that the increase in Sn content cause, as expected, the decrease of the eutectic arrest plateau. Figs. 4 and 5(a and b) show the microstructures commonly present in the alloys under study. It can be observed in these figures the presence of a primary phase, as light grey dendrites surrounded with dark eutectic microconstituent. It can be observed that the increase in Sn content cause, as expected, a decrease in the amount of eutectic.

The experimental cooling curves were numerically processed using the procedures described above. Fig. 6(a) shows the first derivative and zero curves related to 71.5 wt% Sn alloy following all the procedures described previously for zero curve and ts1 procedure. Fig. 6(b) shows the first derivative and zero curves related to 88 wt% Sn alloy following the procedures ZN1, ZN2, ZN3 and ZN4 and ts2 procedure. In these figures it can be seen that depending on the method chosen for the baseline determination there are variations in the related area between the first derivative and the zero Newton baseline curve, which in turn, as will be shown later, will have some effect on the calculated predictions of the amount of microconstituents formed during solidification.

Optical microscopy and image analysis showed, as expected, that the area fractions of eutectic microconstituent decreased with the increase in Sn content. The amount of primary phase determined by image analysis were 0.49 ± 0.015, 0.58 ± 0.02 and 0.84 ± 0.014 for the 71.5 wt% Sn, 77.5 wt% Sn and 88 wt% Sn, Pb–Sn alloys, respectively, and the primary phase solid fractions predicted by the numerical procedures studied in this work and described in Table 2, are shown in Fig. 7(a–c) for the cases under study.

It can be seen in Fig. 7(a and c) that the predictive methods 1–6 considered in this work gives place to amounts of primary phase close to the results obtained from quantitative metallography for the Pb–71.5%Sn and Pb–88%Sn alloys. However, in the case of the Pb–77.5%Sn alloy, Fig. 7(b), the NTA predictions in all cases are far from the observed values of primary phase content.

Another feature that can be observed in Fig. 7 is that the results are almost the same independently of the selection of one of the two procedures considered in this work for t_{ss} determination and the good reproducibility of methods 3–6. Methods 3–6 considers only two points on the first derivative of the cooling curve to generate the zero curve which in turn, as can be seen

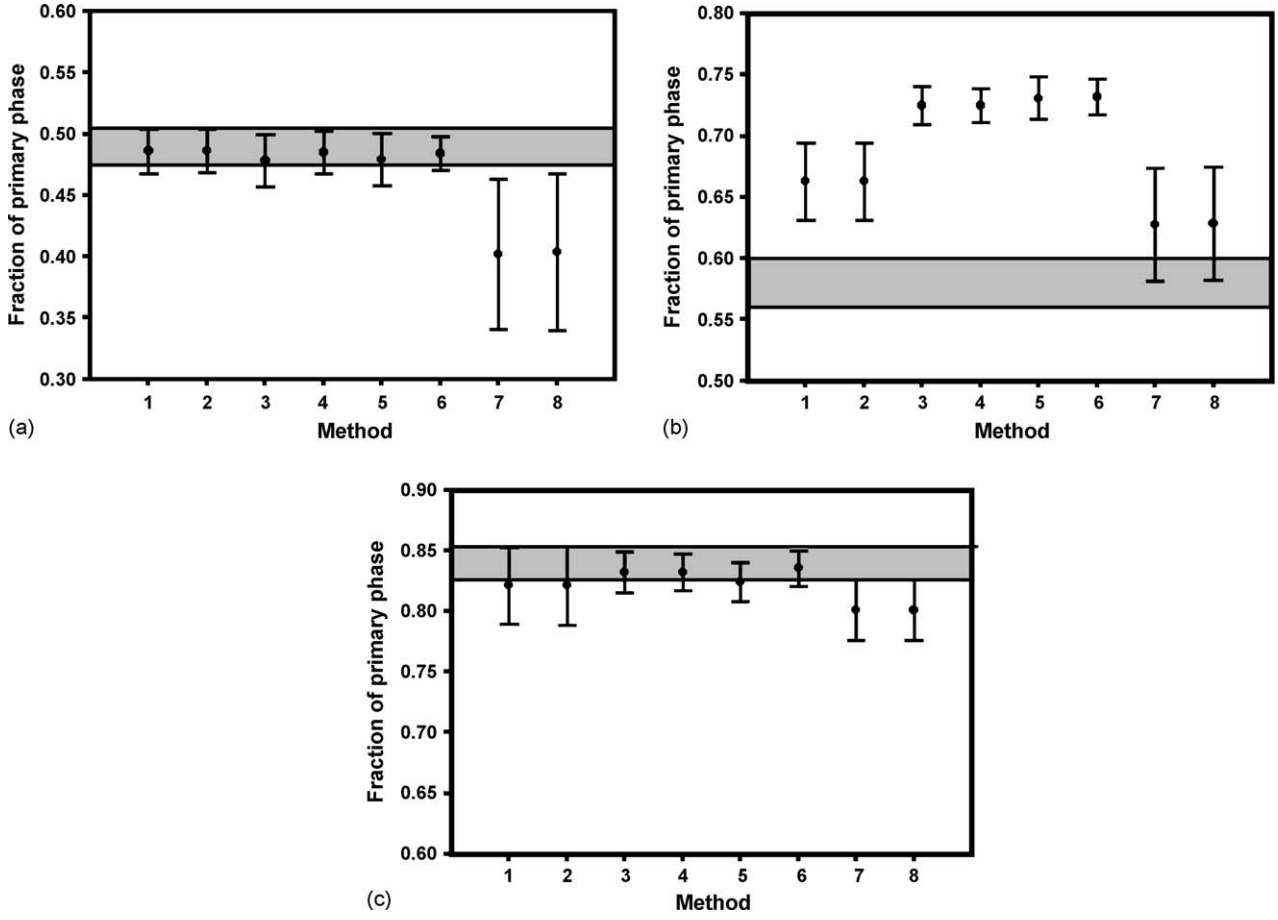

Fig. 7. Amount of primary phase determined by image analysis (dashed zone), and predicted by the numerical procedures studied in this work. (a) Pb–71.5%Sn alloy; (b) Pb–77.5%Sn alloy and (c) Pb–88%Sn alloy.

in Fig. 7, with the experimental conditions present in this work, produce lower dispersions than those associated with the other methods. It can be inferred from the discrepancies observed in Fig. 7(b) that the main drawback of NTA method lies in the arbitrary nature of the zero baseline curve. This in turn produces in some cases results close to the experimental output while in another cases give place to bad predictions, as can be seen in Fig. 7. The same inconsistency has been reported in literatures [2,4] concerning latent heat determinations. It has been shown [3–5] that a more realistic method to generate the zero baseline curve, based on readings of the actual temperature field in the metal can be achieved by the so called Fourier thermal analysis. This feature is the subject of ongoing research by the authors.

Finally, and taking into account the good reproducibility of NTA method in the cases of procedures 3–6 studied in this work for the prediction of the amount of microconstituents formed during solidification, it could be interesting for industrial on-line applications to seek an adjusting factor technique focused to bring the NTA predicted values closer to the experimental results. Further work is needed to exploit the potential benefits offered by Newton thermal analysis technique.

7. Conclusion

The use of Newtonian thermal analysis method for prediction of the amount of microconstituents formed during solidification obtain good results in two of the three cases under study suggesting that this method is not reliable as a tool for quantification of microconstituents.

Acknowledgements

The authors would like to acknowledge to the DGAPA, DGEP (UNAM) and CONACYT for the financial support and to S. García, G. Aramburo, A. Amaro, G. González, I. Puente, I. Beltran and C. Atlatenco for their valuable technical assistance.

References

[1] D. Apelian, J.A. Chang, Al–Si procesing variables: effect on grain refinement and eutectic modification, AFS Trans. 94 (1986) 797–808.
[2] K.G. Upadhya, D.M. Stefanescu, K. Lieu, B.P. Ycager, Computer aided cooling curve analysis: principles and applications in metal casting, AFS Trans. 97 (1989) 61–66.
[3] E. Fras, W. Kapturkisewicz, A new concept in thermal analysis of castings, AFS Trans. 101 (1993) 505–511.
[4] V.O. Barlow, D.M. Stefanescu, Computer aided cooling curve analysis revisited, AFS Trans. 105 (1997) 349–354.
[5] E. Fras, W. Kapturkiewicz, A. Burbielko, H.F. Lopez, Numerical simulation and fourier thermal analysis of the solidification kinetics in high-carbon Fe–C alloys, Metall. Mat. Trans. B 28B (1997) 115–123.
[6] D. Emadi, L.V. Withing, Determination of solidification characteristics of Al–Si alloys by thermal analysis, AFS Trans. 110 (2002) 285–296.
[7] R.I. Mackay, M.B. Djurdjevie, J.A. Sokoloswki, Effect of cooling rate on fraction solid of metallurgical reactions in 319 alloy, AFS Trans. 108 (2000) 521–530.
[8] M.B. Djurdjevic, W. Kasprzak, A. Kierkus, W.T. Kierkus, J.H. Sokolowski, Quantification of Cu enriched phases in synthetic 3XX aluminium alloys using the thermal analysis technique, AFS Trans. 109 (2001) 517–528.
[9] D.R. Poirier, Densities of Pb–Sn alloys during solidification, Metall. Trans. A 19A (1988) 2349–2354.
[10] D.R. Poirier, P. Nandapurkar, Enthalpies of a binary alloy during solidification, Metall. Trans. A 19A (1988) 3057–3061.
[11] W.T. Kierkus, J.H. Solokowski, Recent advances in CCA: a new method of determining baseline equation, AFS Trans. 107 (1999) 161–167.
[12] D. Sparkman, A. Kearney, Breakthrough in aluminum alloy thermal analysis technology for process control, AFS Trans. 102 (1994) 455–460.